ChemComm

Controlled polymerizations using metal–organic frameworks

Journal:	*ChemComm*
Manuscript ID	CC-FEA-08-2018-006415.R1
Article Type:	Feature Article

ChemComm

FEATURE ARTICLE

Controlled polymerizations using metal–organic frameworks

Shuto Mochizuki,[a] Takashi Kitao,[b,c] and Takashi Uemura*[b,c,d]

Received 00th January 20xx,
Accepted 00th January 20xx

DOI: 10.1039/x0xx00000x

www.rsc.org/

This short review focuses on recent developments in polymerization reactions using metal–organic frameworks (MOFs). MOFs are crystalline porous materials that are able to tune their frameworks, enabling their use as promising media for polymerization. The precise design of the MOF structure is key to controlling polymerizations, allowing for the regulation of not only primary but also higher-order structures.

Introduction

Enzymatic polymerizations by biological systems utilize well-tailored nanospaces, and enable the regulation of the chain length and sequence of biopolymers (*e.g.*, DNA, peptides). Inspired by these elegant systems, polymerization reactions imposed by artificial geometrical constraints, such as organic crystals, zeolite, clay, mesoporous silica, and mesoporous alumina,[1-3] have been investigated as a method for controlling the structure of the resulting polymer by through-space interactions.

Recently, metal–organic frameworks (MOFs), which are composed of metal ions and bridging organic ligands, have attracted much attention as a new class of porous materials.[4-6] The distinctive features of MOFs arise from their highly regulated and well-defined framework structures possessing nanochannels with tunable size, shape, dimensionality, and surface environment. Due to their fascinating properties, MOFs have been widely studied for applications including gas storage, separation, sensing, and drug delivery.[7-10] Following a report on the radical polymerization of styrene (St) in a MOF by Uemura *et al.* in 2005,[11] MOFs have been recognized as promising materials for polymerization reactions.

Fig. 1 shows representative examples of the controlled synthesis of polymers using MOFs. Primary and higher-order structures of polymers have been reasonably well regulated by transferring the spatial information of the host MOFs to the monomer units. Moreover, catalytic polymerization by reactive sites in MOFs has exhibited higher conversion efficiency than conventional methods, indicating the usefulness of polymer synthesis using MOFs.

In this feature article, we describe recent developments in polymerization systems using MOF nanochannels for controlling polymer structures and for obtaining ordered macromolecular architectures.

[a] *Department of Synthetic Chemistry and Biological Chemistry, Graduate School of Engineering, Kyoto University, Katsura, Nishikyo-ku, Kyoto 615-8510, Japan.*
[b] *Department of Advanced Materials Science, Graduate School of Frontier Sciences, The University of Tokyo, 5-1-5 Kashiwanoha, Kashiwa, Chiba 277-8561, Japan. E-mail: t-uemura@k.u-tokyo.ac.jp*
[c] *Department of Applied Chemistry, Graduate School of Engineering, The University of Tokyo, 7-3-1 Hongo, Bunkyo-ku, Tokyo 113-8656, Japan.*
[d] *CREST, Japan Science and Technology Agency (JST), 4-1-8 Honcho, Kawaguchi, Saitama 332-0012, Japan.*

Polymerization using MOFs

Since MOFs possess designable crystalline pores, they can be used as tailor-made "nanoflasks" and scaffolds for polymerization reactions. Depending on the objective and reaction conditions, MOFs may be used for controlling polymerizations in either of two ways: (1) polymerizations proceeding only inside the pores and (2) polymerizations propagating from MOFs. Table 1 summarizes the combinations of MOFs and polymers together with the polymerization methods used and the objectives of each system.

Polymerization "within" MOFs

Polymerizations inside the pores of MOFs can be further divided into three categories: (1) polymerization of guest monomers, (2) copolymerization between host and guest monomers, and (3) topochemical polymerization in the MOF.

Method (1) utilizes the confinement effects resulting from regulated nanochannels while exploiting the fact that the behavior of the confined molecules is highly dependent on the structure of the nanospace.[12] Tunable nanospaces of MOFs allow for the regulation of the arrangement, reactivity, and reaction direction of the encapsulated monomers, which is of key importance for the synthesis of polymeric materials with controlled primary structures. It should be noted that a strong confinement effect would reduce the mobility of monomers in the nanochannels, thereby decreasing the monomer reactivity.

Method (2) allows the transcription of the host's ordered structure onto the polymeric products. Depending on the dimensionality of the reaction pathway and the distribution of monomers (or cross-linkers) that have been immobilized into the MOF, the monomer sequence, polymer alignment, and network structures can be precisely regulated.

Method (3) is the topochemical polymerization of polymerizable difunctional ligands or guests in MOFs in a single-crystal-to-single-crystal (SCSC) manner. This method

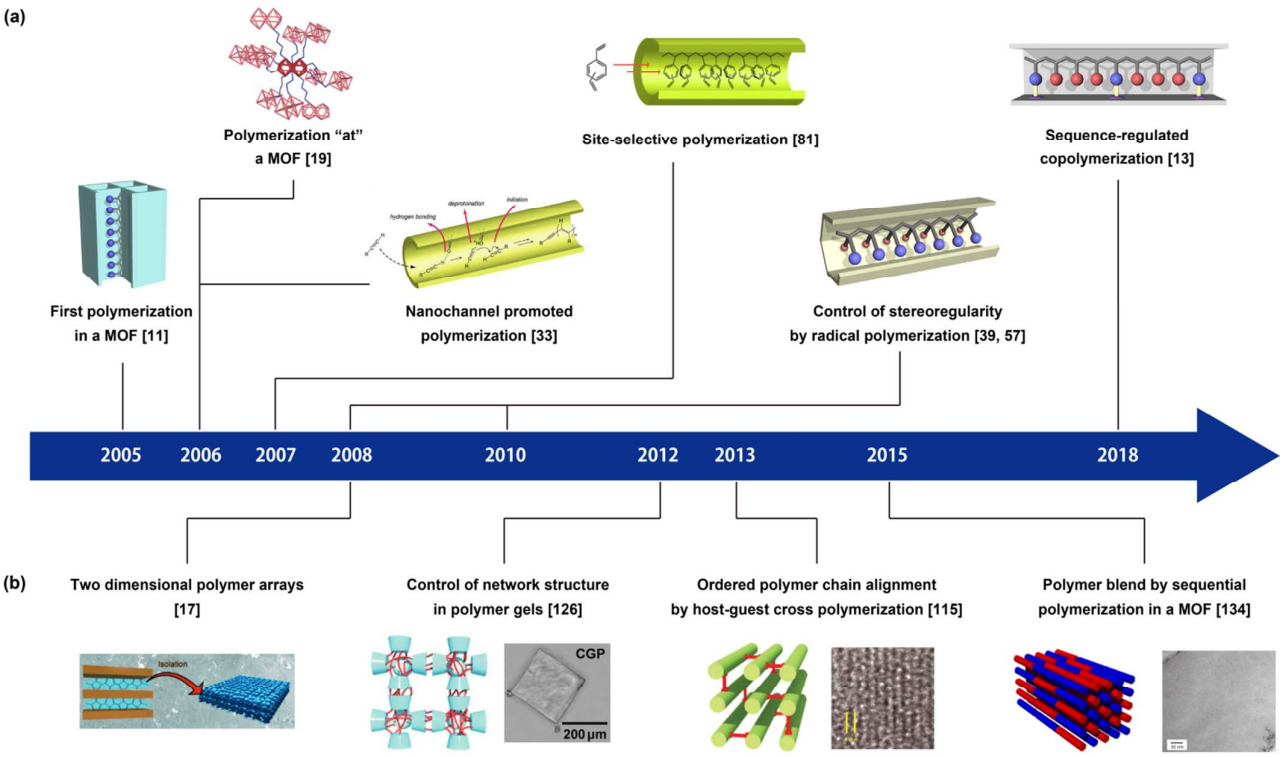

Fig. 1 Timeline of representatives for controlled polymerizations using MOFs. (a) Regulation of primary structures of polymers. (b) Preparation of polymers with controlled higher-order structure.

affords polymers with a precisely controlled stereoregularity; however, it is challenging to arrange the monomer species in suitable positions prior to polymerization.

The confined polymers cannot usually be recovered by solvent extraction because of strong confinement in MOFs. Thus, liberation of the polymers requires the dissolution of the MOF using solutions containing acid, base, and chelating agents. The MOFs can be recycled by recrystallization of the organic linkers and the metal ions after the decomposition process.[13]

Polymerization "at" MOFs

The advantages offered by heterogeneous catalysts over their homogeneous counterparts are recyclability, facile separation from product streams, and often greater thermal stability. Nevertheless, the design and synthesis of new highly active and selective heterogeneous catalysts remain a challenge because heterogeneous catalysts are typically supported on structurally/chemically irregular surfaces such as SiO_2 and Al_2O_3. Thus, the preparation of heterogeneous catalysts in a controlled, well-defined molecular manner is highly desirable.

MOFs are crystalline porous materials that can possess homogeneously distributed reaction sites throughout their structures at metal nodes or ligands, causing them to be recognized as promising candidates for new heterogeneous catalysts.[14-16] The electronically and sterically controllable nature of MOFs enables to exhibit high catalytic selectivity. In catalytic polymerizations using MOFs, both the surface and the interior of the framework can participate during reactions. Furthermore, their insolubility often permits their reuse after polymerization reactions without major loss of catalytic activity.

Polymerization methods

Polymerization mediated by additional polymerization inducers

The simplest method for performing polymerizations using MOFs involves using additional polymerization inducers such as initiators, oxidants, or catalysts. Generally, only a small amount of an inducer is required for the polymerization to proceed. Since the MOF acts only as a scaffold for these reactions, conventional polymerization methods can be easily employed, without modification, provided that the reagents and reaction conditions do not destroy the crystal structures of the MOFs.

Polymerization mediated by preorganized active sites in MOFs

The versatile pore features of MOFs such as Lewis acidity/basicity and redox activity can be precisely tailored by the choice of metal ions and organic ligands. Thus, MOFs bearing active sites in their nanochannels can be envisioned as polymerization activators. For example, oxidative

polymerization mediated by redox-active metal sites in MOFs has been shown to be a viable method for polymerizing pyrrole (Py) in $[(Ni(dmen_2))_2(Fe^{III}(CN)_6)]PhBSO_3$ (dmen = 1,1-dimethylethylenediamine; $PhBSO_3$ = *p*-phenylbenzenesulfonate)[17] and $[Cu_3(btc)_2]_n$ (btc = 1,3,5-benzenetricarboxylate),[18] where Fe^{3+} and Cu^{2+} ions are reduced to Fe^{2+} and Cu^{+} ions, respectively. Titanium alkoxide-based MOFs can also act as initiators for ring-opening polymerizations of ε-caprolactone and L-lactide[19], further demonstrating that the metal sites of MOFs can be used for the synthesis of polymers.

Subsequently, metal sites in MOFs were exploited as catalysts for radical polymerization and coordination polymerization.[20-32] It is the well-defined and homogeneous coordination structures of the MOFs that make them suitable for the creation of specific reaction sites. These sites are formed when the inorganic node undergoes cation exchange with structural retention, offering a predictable strategy to incorporate catalytically active transition metals periodically throughout the system. The result is that MOFs exhibit superior catalytic activity compared with conventional heterogeneous catalysts.

It is also possible to use ligands as active sites for promoting polymerizations. For example, the anionic polymerization of acidic acetylene was initiated by carboxylate groups in $[Cu_2(pzdc)_2(bpy)]_n$ (pzdc = pyrazine-2,3-dicarboxylate; bpy = 4,4′-bipyridine).[33] The IR spectrum of the MOF–monomer composite clearly showed strong interactions between the basic carboxylate oxygen atoms and the acetylene hydrogen atoms. Interestingly, this reaction does not proceed when using sodium benzoate as a discrete model catalyst. This observation provides further support that the arrangement of active sites at appropriate positions along the nanochannels is critically important for spontaneous polymerization to occur. Furthermore, MOF ligands can also act as heterogeneous sensitizers for photopolymerizations, such as the living radical polymerization of vinyl monomers.[34-36] In instances where polymerizable moieties are embedded in the ligands, they can participate in the polymerization as monomers, thereby transcribing the structural periodicity of the MOF to the resulting polymers simply because the position of the ligands is predetermined prior to the polymerization.[13, 37, 38]

Table 1 Summary of the reported controlled polymerizations using MOFs

Chemical formula of MOF[a]	"within" or "at" MOFs	Method	Monomer[a]	Objective	Ref
$[M_2(bdc)_2(ted)]_n$ (M = Cu^{2+}, Zn^{2+})	within	Radical polymerization	St	Molecular weight control	11
$[Cu_2(bdc)_2(ted)]_n$	within	Radical copolymerization	St/MMA, St/VAc	Monomer reactivity ratio	79
	at	Living radical polymerization	BzMA, St, 2-VP, 4-VP, IP, DMAEMA, MMA	Molecular weight control	22, 32
$[Zn_2(bdc)_2(ted)]_n$	within	Radical polymerization	St, MMA	Morphology	102
	within	Radical polymerization	St/MMA, St/A	Polymer blend	134
	within	Living radical polymerization	VAc, VPr, VBu	Molecular weight control	40
	within	Living radical polymerization	MMA, EMA, BzMA, IBMA	Molecular weight control, stereoregularity	57
$[M_2(L)_2(ted)]_n$ (M = Cu^{2+}, Zn^{2+}; L = dicarboxylate ligands)	within	Radical polymerization	DVB	Inhibition of cross-linking	81
	within	Radical polymerization	St, MMA, VAc	Molecular weight control, stereoregularity	39,58
	within	Radical polymerization	DO, AA	Inhibition of cross-linking	82
	within	Radical polymerization	DMB	Inhibition of cross-linking, Stereoregularity	63
$[Cu(dvtp)_x(bdc)_{1-x}(ted)_{0.5}]_n$	within	Radical polymerization	St, MMA	Morphology, polymer chain alignment	115
$[Zn_2(1,4\text{-ndc})_2(ted)]_n$	within	Oxidative polymerization	EDOT	Morphology	105
$[Cu_2(pzdc)_2(bpy)]_n$	within	Anionic polymerization	MP	Stereoregularity, inhibition of cyclization	33
$[M(btb)]_n$ (M = Al^{3+}, Eu^{3+}, Nd^{3+}, Y^{3+}, La^{3+}, Tb^{3+})	within	Radical polymerization	MMA	Stereoregularity	59
$[Nd(btb)]_n$	at	Coordination polymerization	IP	Molecular weight control, stereoregularity	24
$[La(btb)]_n$	within	Radical polymerization	VCz	Morphology	103
	within	Oxidative polymerization	TTh	Morphology, polymer chain alignment	104
	within	Cationic polymerization	AGlu	Inhibition of cross-linking	83
$[Tb(btb)]_n$	within	Radical polymerization	St/MMA	Monomer sequence	80
$[Cu(std)]_n$	within	Radical polymerization	A, MVK	Monomer sequence	13
$[Fe(OH)(bdc)]_n$	at	Living radical polymerization	DMAA, DMAEMA, NHEA, MA	Molecular weight control	47
$[Al(OH)(2,6\text{-ndc})]_n$	within	Radical polymerization	$Fe(\eta\text{-}C_5H_4)_2SiMePh$	Inhibition of cyclization	64
$[Zn_3(D,L\text{-lactate})_2(pyb)_2]_n$	within	Oxidative polymerization	Py	Morphology	107
$[Ti_6O_6(OCH_3)_6(C_{20}H_{14}N_2(CO_2)_2)_3]_n$	at	Living radical polymerization	MMA	Molecular weight control	20
$Ti_6O_{24}C_{90}H_{72}N_6$	at	Living radical polymerization	St, BzMA, MMA	Molecular weight control	21
$[(Ni(dmen_2))_2(Fe^{III}(CN)_6)]PhBSO_3$	within	Oxidative polymerization	Py	Dimensionality	17
$[Co_2(hddip)]\cdot 5DMF$	within	UV-induced polymerization	P_4	Dimensionality	116
$[Cu_3(btc)_2]_n$	within	Cationic polymerization	AGlu	Dimensionality	122
	within	Oxidative polymerization	Py	Dimensionality	18
	within	Oxidative polymerization	L-DOPA	Morphology	108
	within	Electrochemical polymerization	ANI	Morphology, polymer network	106
$Zn_4O[sita\text{-}CrCl_2(THF)_2]_{0.09}(ata)_{2.91}$	at	Coordination polymerization	ET	Molecular weight control	23
M^{n+} exchanged $[Zn_5Cl_4(btdd)_3]_n$ (M^{n+} = Ti^{3+}, Ti^{4+}, Cr^{2+}. Cr^{3+})	at	Coordination polymerization	ET, ET/PR	Molecular weight control	28
Co^{2+} exchanged $[Zn_5Cl_4(btdd)_3]_n$	at	Coordination polymerization	Bu	Molecular weight control, stereoregularity	29
V^{2+} or V^{4+} exchanged $[Zn_5Cl_4(btdd)_3]_n$	at	Coordination polymerization	ET, PR	Molecular weight control, stereoregularity	31
$[Zn(bpeb)(bdc)]\cdot H_2O\cdot 0.1DMA$	within	[2+2] cycloadditon polymerization	bpeb	Stereoregularity	69
$[Zn_2(bpeb)(bdc)(fa)_2]$	within	[2+2] cycloadditon polymerization	bpeb	Stereoregularity	70
$[Zn_2(bpeb)(obc)_2]\cdot 4H_2O$	within	[2+2] cycloadditon polymerization	bpeb	Stereoregularity	71
$[Zr_6O_4(OH)_4(aedb)_6]\cdot 6DMF$	at	Living radical polymerization	MMA, *n*-BuMA, *i*-BuMA, St	Molecular weight control	34
$(Me_2NH_2)[In(aedip)]\cdot 3(H_2O)\cdot 0.5DMF$	at	Living radical polymerization	MMA , *n*-BuMA, *i*-BuMA, St	Molecular weight control	35
$[Zn(bdc)(bpea)]_2\cdot DMF$	at	Living radical polymerization	MMA , *n*-BuMA, *i*-BuMA, St	Molecular weight control	36
$[Zn(mim)_2]_n$ with DhHP-6	at	Living radical polymerization	$PEGMA_{500}$	Molecular weight control	46

$[Ti_2L_3(LH)_2]_n$	at	Coordination polymerization	CAP, L-LA, *rac*-LA	Molecular weight control	19
$[Hf_6(\mu_3\text{-}O)_4(\mu_3\text{-}OH)_4(OH)_4(H_2O)_4(tbap)_2]_n$ treated with $ZrBn_4$	at	Coordination polymerization	ET, Hex	Molecular weight control, stereoregularity	25
$[Zr_6O_4(OH)_4(btc)_2Cl_{12}H_6]_n$	at	Coordination polymerization	ET	Molecular weight control	26
$[(C_{48}H_{80}O_{40})(KOH)_2]_n$	within	Condensation polymerization	EGDE	Polymer network	126
$[Zn_4O(ba\text{-}tpdc)_3]_n$ $[Zn_4O(ba\text{-}bpdc)_3]_n$ $[Cu(ba\text{-}bpdc)_2]_n$ $[Zr_6O_4(OH)_4(ba\text{-}tpdc)_6]_n$	within	Polymerization using click reaction	Diazide ligands (ba-bpdc or ba-tpdc) and tppe	Polymer network	37
$[Cu_2(ba\text{-}tpdc)_2(bpy)]_n$ $[Cu_2(ba\text{-}tpdc)_2(pyz)]_n$ $[Cu_2(ba\text{-}tpdc)_2(ted)]_n$	within	Polymerization using click reaction	ba-tpdc and tppe	Polymer network	38, 127
$[Cu(da\text{-}sbdc)_2]_n$	within	Polymerization using click reaction	da-sbdc and tmetp	Polymer network	128, 130
$[Cu(ba\text{-}tpdc)_2]_n$	within	Polymerization using click reaction	ba-tpdc and tmetp	Polymer network	129
$[Cu(bab\text{-}tpdc)_x(bmb\text{-}tpdc)_{2-x}]_n$	within	Polymerization using click reaction	bab-tpdc	Polymer network	131

[a] See list of abbreviations.

Control of primary structures

Because of the highly designable features of MOFs, the nanochannels of MOFs can be applied as a tailor-made polymerization system to obtain polymers with controlled structures. In this section, we discuss the significant effects of the host framework on the primary structure of the polymer, including the molecular weight, stereoregularity, reaction site, and monomer sequence (Fig. 2).

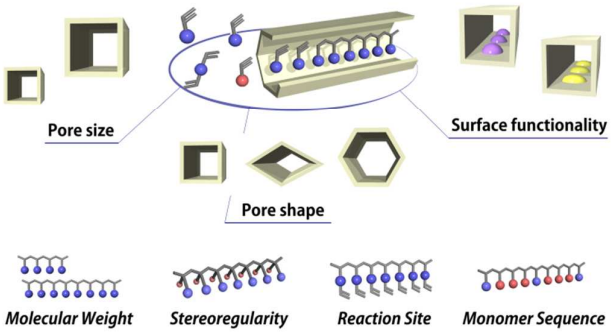

Fig. 2 Schematic illustration of control of the primary structure of polymers synthesized in MOF nanochannels.

Molecular weight

Radical polymerization is the most widely employed process for producing vinyl polymers on both industrial and laboratory scales. In this method, the molecular weight distribution (MWD) is generally broad because termination and chain transfer reactions occur simultaneously with chain propagation. Therefore, suppressing these side reactions is crucial to the production of polymers with narrow MWD. In 2005, the pioneering work of Uemura *et al.* on the radical polymerization of St in the 1D nanochannels of $[Zn_2(bdc)_2(ted)]_n$ (bdc = 1,4-benzenedicarboxylate; ted = triethylenediamine) (Fig. 3)[11] demonstrated that narrow MWD polymers could be produced when the polymerization was performed within the pores. Electron spin resonance measurements during the polymerization revealed that the propagating radicals in this system were highly stabilized in the

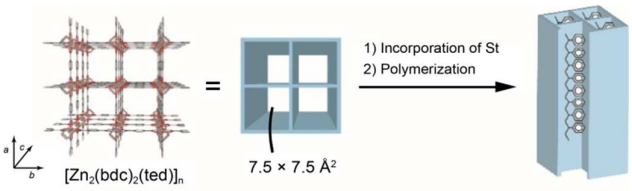

Fig. 3 Schematic illustration of polymerization of St in 1D nanochannels of $[Zn_2(bdc)_2(ted)]_n$. Reprinted with permission from ref. 112. Copyright 2008 American Chemical Society.

MOF nanochannels and resulted in the suppression of radical quenching by termination and chain transfer reactions. Note that the polymerization also proceeded when using the Cu analogue, $[Cu_2(bdc)_2(ted)]_n$. This contrasted with the solution radical polymerization in the presence of Cu^{2+}, likely because the Cu^{2+} ions in the MOF are coordinatively saturated by organic linkers and are protected from being attacked by radical species.

The molecular weight dependency on channel size was studied using $[M_2(L)_2(ted)]_n$ (M = Zn^{2+}, Cu^{2+}; L = dicarboxylate ligand),[39] wherein the pore size can be easily tailored with various dicarboxylate ligands (L). The MWD of polystyrene (PSt) became narrower as the size of the nanochannels decreased, eventually giving a MWD value of 1.5 when using $[Zn_2(1,4\text{-}ndc)_2(ted)]_n$ (ndc = naphthalenedicarboxylate). Other vinyl monomers such as methyl methacrylate (MMA) and vinyl acetate (VAc) were also successfully polymerized in MOFs to yield polymers with low MWD.

The effects of the monomer size on radical polymerizations of vinyl esters in $[Zn_2(bdc)_2(ted)]_n$ were investigated by Hwang *et al.* (Fig. 4).[40] The MWD of poly(vinyl esters) became narrower with an increase in monomer size: 2.17 for poly(vinyl acetate) (PVAc), 1.71 for poly(vinyl propionate) (PVPr), and 1.51 for poly(vinyl butyrate). Moreover, reversible addition–fragmentation chain transfer (RAFT) polymerization[41, 42]—a living radical polymerization technique—was performed in the MOF to demonstrate further control of MWD. This contrasted sharply to the free radical polymerization system. There was a linear molecular weight increase as the reaction time increased. This is clearly indicative of the controlled characteristics of the RAFT polymerization process. The MWDs

of PVAc (1.25) and PVPr (1.34) in the MOF are comparable with their bulk counterparts (1.21 and 1.56, respectively) prepared by RAFT polymerization, and are all significantly lower than those of PVAc (2.17) and PVPr (1.71) prepared by free radical polymerization in the MOF.

Thus far, the focus here has been on the polymerization taking place "within" the MOF. MOFs can also be used as heterogeneous catalysts in polymerizations for controlling the molecular weight of polymers. In solution polymerization systems, living radical polymerization techniques, such as atom transfer radical polymerization (ATRP)[43-45] and RAFT polymerization, are the most studied methods for controlling the molecular weight. Catalysts that are used in these systems generally cannot be reused, and unfavorable coordination of monomers to the catalysts often reduces the catalytic activity. To circumvent these issues, Cu(II) MOFs have been utilized as catalysts for activators regenerated by electron transfer ATRP,[22, 32] MOFs with anthracene ligands have been used as photosensitizers for ATRP,[34-36] Ti(IV)-based MOFs have been utilized as photocatalysts for ATRP,[20, 21] and enzyme mimicking composites have been employed as catalysts for ATRP[46] and RAFT polymerization.[47] MOFs can also be used as catalysts for coordination insertion polymerization. A number of reports demonstrate the high activity and high molecular weight that can be achieved by coordination polymerization of olefins in MOFs.[23-28] Unfortunately, the achievement of both high activity and narrow MWD from a single MOF system for heterogeneous coordination polymerization remains elusive.

Stereoregularity

The stereoregularity (tacticity) of polymers has a great influence on their properties, such as crystallinity, glass transition temperature, melting point, and mechanical strength.[48-50] However, to date, control of stereoregularity during radical polymerization has been extremely challenging due to a lack of efficient methods for the creation of a stereospecific environment around the propagating radical species. For conventional solution polymerizations, several methods that offer stereoregularity control have been reported, *e.g.*, the use of additives such as Lewis acids and polar solvents.[51-53] Polymerization of monomers with extremely bulky substituents and chiral auxiliaries has also emerged as a method to prepare stereoregular polymers.[54-56]

Nanoconfinement effects on stereoregularity have been observed for polymerizations taking place within the nanochannels of MOFs. For example, radical polymerization of vinyl monomers in the 1D nanochannels of $[M_2(L)_2(ted)]_n$ led to an increase in the isotacticity of the resulting polymers.[39] This tacticity is strongly dependent on the pore size of the host and it led to an increase of 9% meso (*m*) diads for poly(methyl methacrylate) (PMMA) when $[Cu_2(1,4\text{-ndc})_2(ted)]_n$ (pore size = 5.7×5.7 Å^2) was used as the host, compared with the bulk system. Because there are no specific interactions between the monomers and the pore walls, this tacticity was attributed to effective through-space interactions by the MOF nanochannels and resulted in the polymer propagation to give

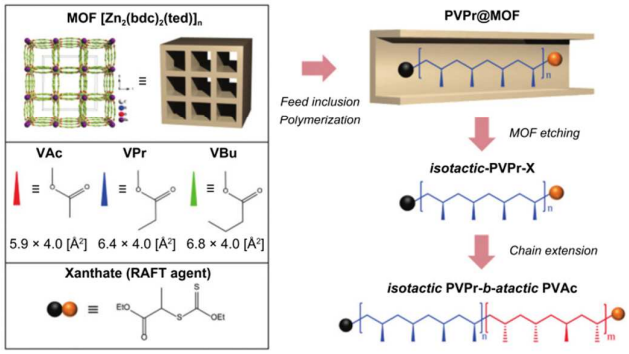

Fig. 4 Schematic illustration of RAFT polymerization in the 1D nanochannels of $[Zn_2(bdc)_2(ted)]_n$. Reproduced from ref. 40 with permission from The Royal Society of Chemistry.

the less stereo-bulky isotactic units. Change in isotacticity was also observed while increasing the size of the substituent groups on guest monomers.[40, 57]

The fraction of isotactic units was further increased through the systematic functionalization of the MOFs by introducing various substituents onto their dicarboxylate ligands.[58] Indications were that the stereoregularity strongly depended on the number and position of the substituents. Polymerization of MMA in $[Cu_2(2,5\text{-dimethoxyterephthalate})_2(ted)]_n$ afforded PMMA with high isotactic and heterotactic triad fractions. This remains one of the most effective systems for controlling the tacticity of PMMA produced by radical polymerization and occurs because the helically twisted channels induce the formation of isotactic-rich polymers, as suggested by molecular dynamics simulations.

More recently, Schmidt's group have demonstrated ATRP and RAFT polymerization inside MOF nanochannels, showing multilevel regulated polymerization via control of tacticity, molecular weight, and end groups.[40, 57]

An analogous method for controlling the tacticity based on using Lewis acids in solution[51-53] has been demonstrated using MOFs with unsaturated metal sites (UMS) to perform a stereocontrolled polymerization of polar vinyl monomers.[59] In the 1D nanochannels of $[M(btb)]_n$ (M = Al^{3+}, Eu^{3+}, Nd^{3+}, Y^{3+}, La^{3+}, and Tb^{3+}; btb = 1,3,5-benzentrisbenzoate), UMS are located at the corners of the hexagonal channels, and the PMMA tacticity is directly dependent on how strongly the MMA interacts with these UMS. Tb^{3+} embedded in $[Tb(btb)]_n$ effectively induced the stereospecific chain growth of PMMA although discrete Tb^{3+} ions are ineffective in changing the stereoregularity of PMMA.

The polymerization of conjugated diene monomers produces polymers with different stereo- and regiostructures, specifically *trans*-1,4, *cis*-1,4, and 1,2 addition sequences, depending on the method of coordination polymerization that is employed.[60] MOFs have been utilized as precatalysts for the stereoselective coordination polymerization of conjugated diene monomers.[24, 29] Recently, Dubey *et al.* reported that Co-exchanged $[Zn_5Cl_4(btdd)_3]_n$ (H_2btdd = bis(1*H*-1,2,3-triazolo[4,5-*b*],[4′,5′-*i*])dibenzo[1,4]dioxin) works as a highly selective catalyst for the *cis*-1,4-polymerization (>99%) of 1,3-butadiene

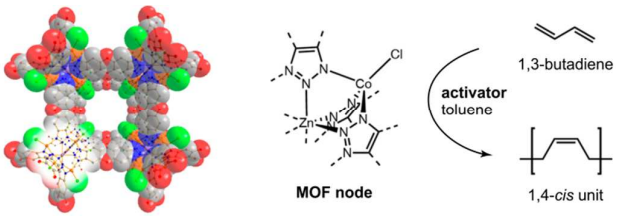

Fig. 5 Stereoselective coordination polymerization of 1,3-butadiene using a Co(II)-exchanged $[Zn_5Cl_4(btdd)_3]_n$ as a heterogeneous catalyst. Reprinted with permission from ref. 29. Copyright 2017 American Chemical Society.

(Fig. 5).[29] The tris-pyrazolylborate-like coordination of Co(II) in the MOF is suitable for stereoinduction, and its discrete, single-site structure gives the highest stereoselectivity for the polymerization of 1,3-butadiene with a heterogeneous catalyst. Whereas coordination polymerization affords stereo- and regiocontrolled polybutadienes, radical polymerization typically gives polymers with uncontrollable primary structures.[61] Moreover, 1,3-butadienes with a substituent group on the 2-position suffer from extremely low polymerization rates under radical conditions due to the large steric hindrance for chain growth and/or unfavorable side reactions.[62] These problems are solved when $[Cu_2(L)_2(ted)]_n$ is employed as the host, allowing the polymerization of 2,3-dimethyl-1,3-butadiene (DMB) to proceed in high yield and with high molecular weight polyDMBs, probably due to the remarkable stabilization afforded to the propagating radicals within the nanochannels.[63] Furthermore, an increase in the *trans*-1,4-addition sequence (*trans*-1,4:*cis*-1,4:1,2 = 70:25:5) was achieved by the functionalization of L in the MOF.

The effect of nanochannels on the tacticity of polymers was also observed for the ring-opening polymerization of an unsymmetrically substituted [1]ferrocenophane monomer.[64] As in the case of vinyl polymers produced in MOFs, the isotacticity (*mm*) of the corresponding polymer increased with decreasing pore diameter of the host MOFs.

Topochemical solid-state polymerization affords materials otherwise difficult to synthesize by conventional organic synthetic methodologies.[65-67] Crystalline stereoregular polymers have been synthesized by the solid-state polymerization of diacetylenes and diolefines, for example.[68] Vittal *et al.* reported a method for the topochemical polymerization in MOFs mediated by [2+2] photocycloaddition of the slip-stacked conjugated diene ligand (1,4-bis[2-(4′-pyridyl)ethenyl]benzene; bpeb) (Fig. 6a).[69, 70] Isotactic polymers were obtained from bpeb with *trans*, *trans*, *trans* conformation in a SCSC manner. The key to this system's success is the formation of infinite slip-stacked assemblies of two C=C bonds in the MOF. A syndiotactic polymer was formed from bpeb ligands with *trans*, *cis*, *trans* conformation.[71] A threefold interpenetrated pillared-layer MOF $[Zn_2(bpeb)(obc)_2]_n \cdot 4H_2O$ (obc = 4,4′-oxybis(benzoate)) was prepared that contains bpeb ligands with all *trans* conformation and an olefin–olefin bond distance of 4.8 Å between the bpeb ligands, rendering them photo-inactive, based on Schmidt's criteria.[72] Interestingly, UV irradiation induces conformational changes to the bpeb ligands, isomerizing them from all *trans* to *trans–cis–trans*. This brings the olefin bonds closer together (within 4.2 Å), and allows polymerization of the bpeb to proceed to give $[Zn_2(S\text{-poly-bpppcb})_{0.5}(obc)_2] \cdot 2.5H_2O$ in which S-poly-bpppcb is a syndiotactic 1,3-(4,4′-bipyridyl)-2-phenylcyclobutane polymer (Fig. 6b).

Topochemical polymerizations of guest molecules in a MOF were realized by Yang *et al.*, where bpeb was incorporated into the MOF as a guest.[73] Subsequent SCSC regioselective photopolymerization via [2+2] photodimerization of the guest proceeded and resulted in the formation of the corresponding isotactic polymer.

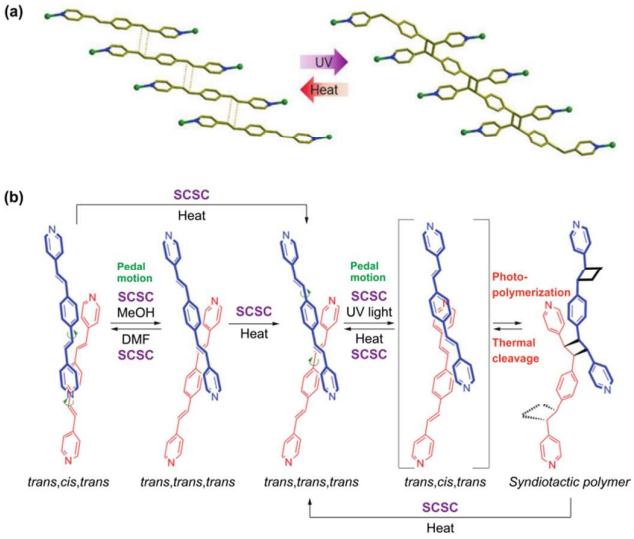

Fig. 6 Topochemical polymerizations using MOFs. (a) Polymerization by [2+2] photocycloaddition of slip-stacked bpeb ligands in a MOF and depolymerization of the resultant polycyclobutanes. Adapted with permission from ref. 69. Copyright 2014 Wiley-VCH. (b) Schematic diagram illustrating various SCSC conversions involving bpeb ligands for forming syndiotactic polymers. Adapted with permission from ref. 71. Copyright 2015 Wiley-VCH.

Monomer sequence and copolymer composition

Control of the monomer composition and sequence is of significant importance for tuning the properties of copolymers. In radical copolymerization, copolymer compositions and sequence distributions are determined by the monomer reactivity ratios.[74] Several examples for making simple periodic sequences have been reported using additives[75] and small template molecules.[76-78] However, copolymerization in nanoporous materials has been much less studied than in homopolymerization counterparts, and the effects of the nanospaces on the diffusion and reactivity of monomers remain unclear.

The first report of copolymer formation in MOFs involved the radical copolymerization of St with MMA in the 1D nanochannels of $[Cu_2(bdc)_2(ted)]_n$.[79] This resulted in

copolymers with high molecular weights (M_w >30,000). The monomer reactivity ratios of St (r_{St}) and MMA (r_{MMA}) were calculated to be 0.39 and 0.72, respectively. The monomer reactivity ratios deviated from those in bulk and solution polymerization systems (r_{St} = 0.53, r_{MMA} = 0.49), probably because the reactivity of St toward the polymer chain terminals is more restricted in the nanochannels than MMA due to its larger molecular size. This phenomenon was also observed for the radical copolymerization of St with VAc in the MOF.[79]

Radical copolymerization of St with MMA was also performed in $[Tb(btb)]_n$.[80] Interaction of MMA with the UMS of the MOF increased the reactivity of the MMA, and there was a drastic increase in the proportion of MMA units in the resulting copolymers compared with that obtained from the corresponding solution polymerization system. However, the inadequate spatial arrangement of monomers in the nanochannels rendered sequence regulation in the resulting copolymers unsuccessful.

Sequence control in radical copolymerization was finally achieved using the periodic structure of a MOF as a template.[13] This was carried out by employing a three-step strategy: (1) preimmobilization of vinyl monomer (X) at regular intervals along the nanochannels of a MOF (MOF⊃X), (2) incorporation of another vinyl monomer (Y) into the MOF to create a host–guest composite [MOF⊃(X+Y)], and (3) copolymerization of the monomers in the composite followed by the removal of the host framework (Fig. 7a). $[Cu(std)]_n$ (std = styrene-3,5-dicarboxylate) was prepared by the self-assembly of styryl ligands, S (styrene-3,5-dicarboxylic acid), with Cu ions for the template. Polymerizable styryl groups are covalently attached throughout the surface of the hexagonal nanochannels, taking up a periodic arrangement along the channel direction (Fig. 7b). The styryl groups were copolymerized with guest acrylonitrile (A), followed by the removal of the template to give the resulting copolymer. The A/S ratio in the copolymer (A/S = 3.0/1.0) was independent of the initial feedstock A/S ratios, indicating the formation of a SAAA periodic sequence in the generated copolymers. Detailed NMR studies indicated the predominant formation of AAA, AAS, and ASA triads, and theoretical calculations supported the formation of a repetitive SAAA sequence in the copolymer. This is the first example of polymerizations in which the structural periodicity of a MOF was precisely transcribed into products on the molecular level.

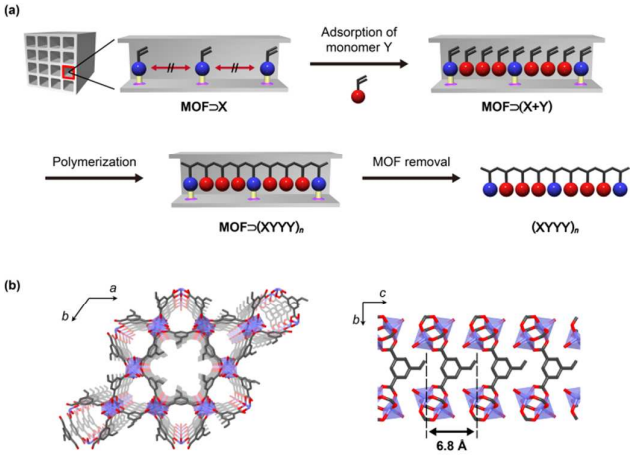

Fig. 7 (a) Schematic illustration of sequence-regulated radical copolymerization using a MOF. (b) Nanochannel structure of $[Cu(std)(H_2O)]_n$. H atoms and one of the disordered vinyl moieties are omitted for clarity. Reprinted from ref. 13 with permission from Macmillan Publishers Ltd: *Nat. Commun.*, copyright 2018.

Inhibition of cross-linking and end-to-end cyclization

Chain-growth polymerization of monomers with multireactive sites usually yields insoluble polymers with a mix of linear, cyclic, and cross-linked structures. Thus, the development of polymerization methods for making soluble linear polymers with reactive sites in a controlled manner is of great importance. Polymerization of *m*-divinylbenzene (*m*-DVB) in $[M_2(bdc)_2(ted)]_n$ (M = Zn^{2+} and Cu^{2+}) yielded soluble linear poly(*m*-DVB).[81] Alternatively, when *p*-divinylbenzene (*p*-DVB) (molecular dimensions = 8.5×4.4 $Å^2$) was employed in the same hosts, the adsorption and polymerization properties of the monomer were affected by the host, such that *p*-DVB induced a lattice expansion in $[Zn_2(bdc)_2(ted)]_n$ compared with the original host, allowing the effective adsorption of the monomer. Conversely, the isostructural copper MOF $[Cu_2(bdc)_2(ted)]_n$ did not show such structural change, leading to less adsorption of *p*-DVB. (The number of *p*-DVB molecules per unit cell in the Zn- and Cu-MOF was 2.0 and 0.9, respectively.) As a result, poly(*p*-DVB) could only be obtained from $[Zn_2(bdc)_2(ted)]_n$. Furthermore, an insoluble polymer product was obtained when using a MOF with a larger channel size. These results indicate that a suitable monomer arrangement to promote single polymer growth in the channels is essential for selective linear polymerization (Fig. 8).

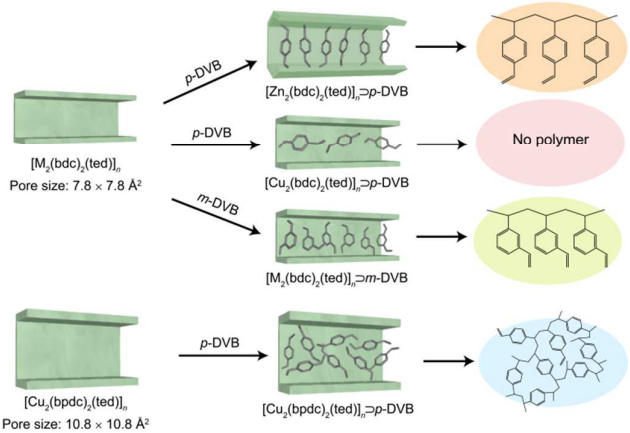

Fig. 8 Schematic illustration of the site-selective radical polymerization of DVBs in MOFs. Adapted with permission from ref. 81. Copyright 2007 Wiley-VCH.

The strategy to suppress cross-linking using MOFs could be applied to the ring-closing polymerization of unconjugated 1,6-diene monomers such as dimethyl 2,2′-[oxybis(methylene)]diacrylate and acrylic anhydride.[82] The unfavorable interpolymer cross-linking was suppressed in the narrow nanochannels of $[Cu_2(bdc)_2(ted)]_n$ to afford soluble linear polymers while polymerization in a MOF with larger pores and in the bulk state gave insoluble polymer products.

Linear polymerization of a cyclic glucose (1,6-anhydro-*β*-*D*-glucose) was demonstrated using the 1D nanochannels of $[La(btb)]_n$. Because cyclic glucose has many reactive hydroxyl groups, cationic ring-opening polymerization of the monomer usually yields highly branched polymers with tri-, tetra-, and pentajunction units. Polymerization of the cyclic glucose monomer in $[La(btb)]_n$ proceeds only along the channel direction, affording a quasilinear polyglucose with no penta- and tetrajunctions.[83] This results in improved solubility and thermal stability of the quasilinear polyglucose compared with the hyperbranched polyglucose.

It is noteworthy that unfavorable cyclization reactions can be prohibited during the course of polymerizations in MOFs. For example, ring-opening polymerization of unsymmetrically substituted [1]ferrocenophane in MOFs with 1D channels only afforded linear polymers while polymerization without MOFs gave both linear and cyclic polymers due to backbiting reactions.[64] In a similar manner, cyclic trimerization of substituted acetylene, methyl propiolate (MP), was suppressed in the nanopores of $[Cu_2(pzdc)_2(bpy)]_n$, producing only a linear poly(MP).[33]

Control of higher-order structure

The higher-order structure of polymers largely governs their physical properties.[84-86] MOFs possess continuous ordered pores over their entire crystal structure and the dimensionality of pores is exactly defined. Confinement of polymers in such pores gives a polymer assembly reflecting the pore connectivity of MOFs. Since host MOFs can be removed under mild conditions, polymer assemblies can be retained during the removal process, leaving polymers with controlled higher-order structure (Fig. 9).

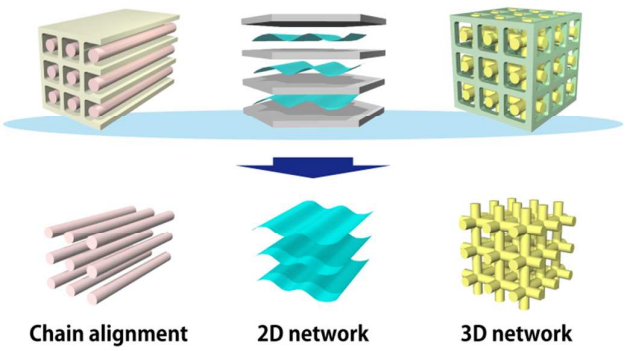

Fig. 9 Schematic illustration of the control of the higher-order structure of polymers

Morphology of polymer particles

The size and shape of polymer particles have a great impact on their properties, well beyond their chemical composition.[87-90] As such, the transfer of size and shape from host materials to their guests is a simple yet versatile method to control the morphology of polymer particles.[91-93] Due to their controlled and finely tuned crystal size and morphology,[94-97] MOFs can be regarded as excellent porous templates for the production of well-defined polymer particles. In particular, anisotropic polymer particles have both theoretical significance and practical applications in the fields of photonic crystals, optoelectronics, and sensors, as well as providing a platform for new phenomena and materials.[98-100] However, polymer particles are usually prepared as spherical beads by suspension, dispersion, and emulsion polymerization methods.[87, 90, 101]

PSt particles with cubic, rod-like, and hexagonal shapes were obtained through the selective dissolution of similar shaped $[Zn_2(bdc)_2(ted)]_n$ as the host.[102] Although the polymer chains were not stabilized by cross-linking, a perfect shape transcription was observed during the isolation process because of the inherent rigidity of PSt, whose glass transition temperature is much higher (105 °C) than room temperature. Moreover, polymer particles obtained by this MOF-based method possessed meso- and macropores which were likely caused by the removal of the host framework as well as unreacted monomers from the original composite. Morphological control has also been achieved for photoconductive polymers (polyvinylcarbazole[103]) and conjugated polymers (polythiophene (PTh),[104] poly(3,4-ethylenedioxythiophene),[105] polyaniline (PANI),[106] and polypyrrole (PPy)[107]). Also, a polymer thin film was fabricated by exploiting surface-mounted MOF (SURMOF) as a template.[108]

1D and 2D ordered polymer alignment

Linear polymers are intrinsically anisotropic and the properties that depend on this anisotropy can be amplified by polymer chain alignment. Unfortunately, vinyl polymers typically have an amorphous phase in their bulk state due to the highly disordered and random entanglement of polymer chains. Several strategies have been utilized to control the alignment of the chains, including mechanical rubbing, magnetic fields, and electrospinning.[109-111] However, these conventional methodologies often lack generality and are unable to maintain the polymer chain alignment permanently.

The confinement of polymers in MOFs is a simple yet effective method to align the polymer chains within the pores.[112-114] In this regard, the maintenance of the chain organization after the removal of the host matrix is a prerequisite for effective polymer chain alignment.

Remarkably, the chain orientation of PTh is not significantly disturbed during the isolation process from a MOF matrix because of its rigid backbone structure, as confirmed by selected area electron diffraction patterns of PTh particles.[104] The obtained PTh particles exhibited higher conductivity than

PTh prepared by solution polymerization due to the extended conjugation system.

Unlike rigid polymers, chain disorder can be easily induced in flexible nonconjugated polymers. Distefano *et al.* elucidated a strategy that relies on "ordered cross-links" in the framework to achieve the uniaxial chain alignment of amorphous vinyl polymers (Fig. 10).[115] $[Cu_2(bdc)_2(ted)]_n$ with 1D nanochannels was used as a structural motif, wherein the bdc in the host was partially replaced by a polymerizable ligand, 2,5-divinyl-terephthalate (dvtp). During the course of polymerization, polymer chains at adjacent channels are cross-linked by the divinyl species, and thus ordered alignment of the polymer can be maintained even after the removal of the host MOF. Different from the amorphous nature of linear PSt recovered from nonfunctionalized $[Cu_2(bdc)_2(ted)]_n$, the PSt obtained by host–guest cross-polymerization showed a diffraction peak that was assigned to the chain–chain packing structure, and high-resolution TEM images clearly demonstrated the alignment of PSt chains. The density of the cross-linked PSt was therefore much higher than that of conventional PSt materials, which was comparable to the density of ideal 100% crystalline isotactic PSt.

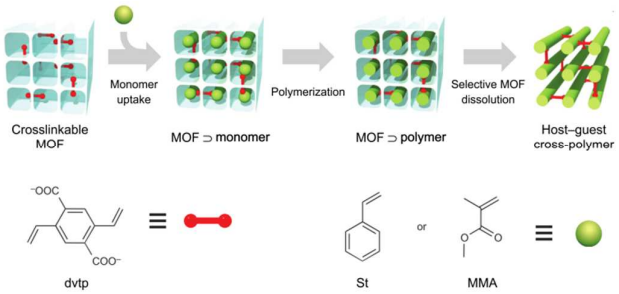

Fig. 10 Schematic illustration of host–guest copolymerization to afford highly ordered cross-linked polymers. Reprinted from ref. 115 with permission from Macmillan Publishers Ltd: *Nat. Chem.*, copyright 2013.

A MOF-mediated strategy also enables the fabrication of 2D ordered arrays of polymer sheets.[17] Intercalative and oxidative polymerization of Py was performed within a redox-active layered MOF and resulted in intercalated PPy microplates after the removal of the host framework with Na-EDTA. The conductivity of the composite parallel to the sheet was found to be 20 times higher than that perpendicular to the sheet. This is a phenomenon that is clearly indicative of a 2D-oriented organization of PPy. Very recently, Li *et al.* reported the confined polymerization of phosphorous in a 2D MOF wherein the resulting thickness of the exfoliated polymer was ~2 nm, corresponding to the interlayer distance of the MOF.[116] These results clearly demonstrate that the MOF template approach can provide a powerful alternative route for producing nanomaterials with 2D ordering at the molecular level.

Controlled polymer networks

It is difficult to construct highly ordered networks in polymeric materials through solution polymerization because the cross-linking points are randomly formed as the reaction proceeds. One of the striking features of MOFs is the well-defined dimensionality of their networks and nanochannels, which can be harnessed to restrict the reaction direction and cross-linking structure to afford polymers. In this regard, the 3D nanochannels of MOFs can be exploited as templates for fabricating porous polymers with controlled pore sizes. Preparation of conducting and porous polymers with defined structures has recently attracted interest due to their potential for applications including sensors, photovoltaics, and supercapacitors.[117-119] Chemical oxidative polymerization of Py was performed within the 3D nanochannels of $[Cu_3(btc)_2]_n$ using the Cu(II) sites on the pore surface.[18] In this case, the IR spectrum of PPy indicated that the cross-linking proceeded during the polymerization process, and the PPy liberated from the MOF showed clear adsorption properties, in great contrast to PPy prepared using bulk conditions. Lu *et al*. reported on the electropolymerization of aniline (ANI) inside $[Cu_3(btc)_2]_n$.[106] They demonstrated that PANI with a high porosity (S_{BET} = 986 m^2/g) and uniform pore size distribution centered around 0.84 nm could be produced, probably because of the high cross-linking density. The adsorption characteristics were in good agreement with the size of the Cu paddlewheel clusters in $[Cu_3(btc)_2]_n$.

As porous polysaccharides can be expected to serve as drug carriers, due to their biocompatibility, many attempts have been made to control their pore and particle sizes.[120, 121] Ring-opening polymerization of 1,6-anhydro glucose in $[Cu_3(btc)_2]_n$ followed by the removal of the host frameworks afforded polysaccharide particles that replicated their MOF templates,[122] showing high mesoporosity, which could be systematically tuned depending on the polymerization conditions. In addition, the porous polysaccharides were capable of loading and releasing drug and protein molecules due to their large specific surface area.

To impart the ordered structures from MOFs on polymer composites, several research groups have focused on the *in situ* cross-linking of ligands, followed by the hydrolysis of coordination bonds. Polymer gels are 3D polymer networks swollen in solvents and they can be used as structural materials and scaffolds for tissue regeneration.[123, 124] Network homogeneity affects the physical properties of polymer gels, such as the mechanical and optical properties.[125] Cross-linking between MOF ligands allows the resulting gel to retain the structure of the original framework with a homogeneous distribution of cross-linking points. Furukawa *et al.* demonstrated the cross-linking of hydroxy and alkoxide groups of γ-cyclodextrin (CD) in a CD-MOF to form a network of polymer particles with well-defined polyhedral shapes.[126] The azide–alkyne click reaction has also been applied to cross-link the ligands in the voids of MOFs (Fig. 11),[37] to give gels that swelled isotropically when immersed in solvent, due to their high reticulation. More recently, the same research group prepared anisotropic polymer gels with axis-dependent cross-linking density originating from the anisotropic arrangement of the organic ligands in pillared-layer MOFs.[38,127]

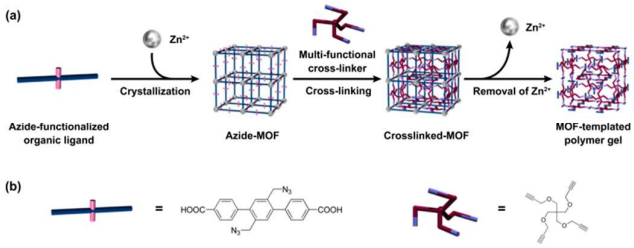

Fig. 11 Schematic illustration of the formation of polymer gels using MOFs as templates. (a) Copolymerization of the organic ligand in a MOF with guest cross-linker followed by subsequent decomposition of the MOF to obtain a polymer gel. (b) Molecular structures of the organic ligand and the cross-linker. Reprinted with permission from ref. 37. Copyright 2013 American Chemical Society.

Similarly, Wöll's group converted highly ordered surface-mounted MOFs (SURMOFs) prepared via liquid phase epitaxy to polymer gel coatings through cross-linking of the linkers.[128-130] The surface-grafted gels had a high porosity and homogeneous thickness, and could be further loaded with bioactive compounds and applied as bioactive coatings, providing a drug release platform for *in vitro* cell culture studies.

Interwoven polymers are much more flexible than network polymers with covalently cross-linked points. This is because their polymer chains can slide relative to each other and thereby distribute forces more easily. It has recently been demonstrated that the polymerization of ligands that are preoriented within SURMOF structures can lead to the formation of linear and interwoven polymer chains (Fig. 12). Using layer-by-layer techniques, polymerizable linkers can be embedded in a nonreactive SURMOF. Notably, the thickness of the interwoven polymer network can be controlled by changing the number of active layers in the SURMOF.[131]

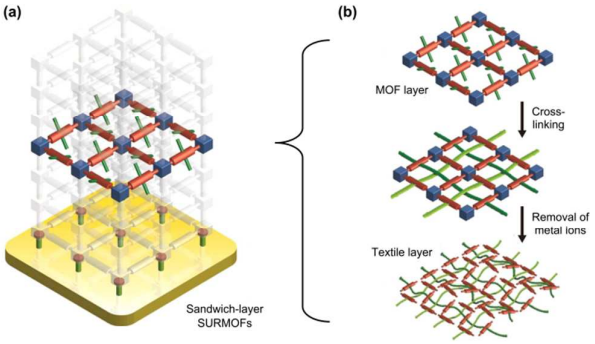

Fig. 12 Schematic illustration of the heteroepitaxial sandwich-layer SURMOF system (a) and the formation procedure of molecular weaving in the active MOF layer embedded between two sacrificial layers (b). Reprinted from ref. 131 with permission from Macmillan Publishers Ltd: *Nat. Commun.*, copyright 2017.

Polymer blends

Because the homogeneous mixing of chemical substances is crucial in most aspects of chemistry, much effort has been devoted to the compatibilization of polymers with the aim to produce new materials with tailored properties.[132, 133] Unfortunately, unlike for low molecular weight compounds, the entropy of mixing for macromolecules is inherently very low; therefore, the mixing of two or more polymers often results in phase separation on the macroscopic scale. Uemura *et al.* solved this problem by using MOFs as a removable template, and achieved the compatibilization of immiscible polymers at the molecular level (Fig. 13).[134] The immiscible polymer pair of PSt and PMMA was prepared via successive homopolymerizations of their monomers in $[Zn_2(bdc)_2(ted)]_n$ to distribute the polymers inside the MOF particles. Subsequent dissolution of the MOF in a Na-EDTA aqueous solution afforded a PSt/PMMA blend that is homogeneous in the range of several nanometers. The kinetically trapped PSt/PMMA blend was sufficiently stable to maintain the mixed state for >8 months at room temperature. Moreover, the polymer blend showed higher thermal stability than the conventional physical blends.

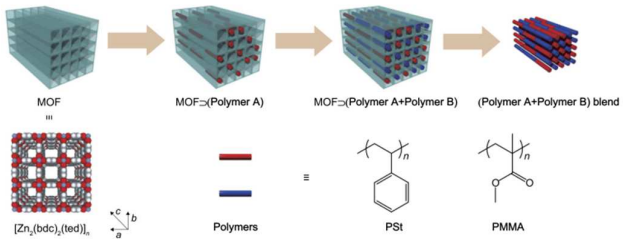

Fig. 13 Preparation of polymer blends using MOF as a template. Reprinted from ref. 134 with permission from Macmillan Publishers Ltd: *Nat. Commun.*, copyright 2015.

Conclusion

In this feature article, we have described the progress of controlled polymerization reactions using MOFs. This technique provides a different approach from conventional polymerizations in bulk and solution phases to regulate polymer structures. Precision control in the micro and macro structure of polymers by MOFs has attracted much attention, and is expected to find use in industrial applications. Cost reduction is one of the biggest issues to be solved, but we assume that the barrier for using these methodologies in industrial applications is not significantly high as the recyclability of MOFs is getting recognized recently for both polymerizations "within" and "at" MOFs. MOF-induced polymerization of synthetic monomers provides a potential route for realizing the laboratory evolution of well-defined polymers with structure regulation at multiple levels. We foresee that the application of MOFs for polymerizations will continue to diversify, bringing new concepts to the field of polymer chemistry.

List of abbreviations

A: acrylonitrile
AA: acrylic anhydride
aedb: 4,4′-(anthracene-9,10-diylbis(ethyne-2,1-diyl))dibenzoate
aedip: 5,5′-(anthracene-9,10-diylbis(ethyne-2,1-diyl))diisophthalate
AGlu: 1,6-anhydro-β-*D*-glucose
ANI: aniline
ata: 2-aminoterephthalate
ATRP: atom transfer radical polymerization
ba-bpdc: bis(azidomethyl)biphenyldicarboxylate
bab-tpdc: bis(acetylene-biphenyl)terphenyl dicarboxylate
ba-tpdc: bis(azidomethyl)terphenyl dicarboxylate
bdc: 1,4-benzenedicarboxylate
bmb-tpdc: bis(methyl-biphenyl)terphenyl dicarboxylate
bpea: 9,10-bis(4′-pyridylethynyl)anthracene
bpeb: 1,4-bis[2-(4′-pyridyl)ethenyl]benzene
bpy: 4,4′-bipyridine
btb: 1,3,5-benzentrisbenzoate
btc: 1,3,5-benzenetricarboxylate
Bu: 1,3-butadiene
BzMA: benzyl methacrylate
CAP: ε-caprolactone
CD: cyclodextrin
da-sbdc: diazido-stilbenedicarboxylate
DhHP-6: deuterohemin-β-Ala-His-Thr-Val-Glu-Lys
DMA: *N*,*N*-dimethylacetamide
DMAA: *N*,*N*-dimethylacrylamide
DMAEMA: 2-(dimethylamino)ethyl methacrylate
DMB: 2,3-dimethyl-1,3-butadiene
dmen: 1,1-dimethylethylenediamine
DMF: *N*,*N*-dimethylformamide
DO: dimethyl 2,2′-[oxybis(methylene)]diacrylate
DVB: divinylbenzene
dvtp: 2,5-divinyl-terephthalate
EDOT: 3,4-ethylenedioxythiophene
EGDE: ethylene glycol diglycidyl ether
EMA: ethyl methacrylate
ET: ethylene
fa: formate
hddip: 5,5′-(hexa-2,4-diyne-1,6-diylbis(oxy))diisophthalate
Hex: 1-hexene
H_2btdd: bis(1*H*-1,2,3-triazolo[4,5-*b*],[4′,5′-*i*])dibenzo[1,4]dioxin
IBMA: isobornyl methacrylate
i-BuMA: *i*-butyl methacrylate
IP: isoprene
L-DOPA: 3,4-dihydroxy-L-phenylalanine
LH_2: 1,4-butanediol
L-LA: L-lactide
m: meso
NHEA: *N*-hydroxyethyl acrylamide
MA: methyl acrylate
mim: 2-methylimidazolate
MMA: methyl methacrylate
MP: methyl propiolate
MVK: methyl vinyl ketone
MWD: molecular weight distribution
n-BuMA: *n*-butyl methacrylate
ndc: naphthalenedicarboxylate
obc: 4,4′-oxybis(benzoate)
PANI: polyaniline
$PEGMA_{500}$: poly(ethylene glycol) methyl ether methacrylate, $M_w = 500$ g/mol
$PhBSO_3$: *p*-phenylbenzenesulfonate
PR: propylene
PVAc: poly(vinyl acetate)
PVPr: poly(vinyl propionate)
PPy: polypyrrole
Py: pyrrole
pyb: 4-pyridylbenzoate
pyz: pyrazine
pzdc: pyrazine-2,3-dicarboxylate
rac-LA: *rac*-lactide
RAFT: reversible addition–fragmentation chain transfer
SCSC: single-crystal-to-single-crystal
sita: 2-salicylideneimine terephthalate
St: styrene
std: styrene-3,5-dicarboxylate
SURMOFs: surface-mounted MOFs
tbap: 1,3,6,8-tetrakis(*p*-benzoate)pyrene
ted: triethylenediamine
THF: tetrahydrofuran
tmetp: trimethylolethane tripropiolate
tppe: tetrapropargyl pentaerythritol
TTh: terthiophene
UMS: unsaturated metal site
VAc: vinyl acetate
VBu: vinyl butyrate
VCz: *N*-vinylcarbazole
VP: vinylpyridine
VPr: vinyl propionate
$ZrBn_4$: tetrabenzylzirconium

Conflicts of interest

There are no conflicts to declare.

Acknowledgements

This work was supported by the JST, CREST program (JPMJCR1321), and a Grant-in-Aid for Science Research on Innovative Area “Coordination Asymmetry” (JP16H06517) from the Ministry of Education, Culture, Sports, Science and Technology, Government of Japan. Additionally, the authors are grateful to Dr Michael MacLean for his help in the editing of this manuscript.

References

1. K. Tajima and T. Aida, *Chem. Commun.*, 2000, 2399-2412.
2. A. Matsumoto, *Polym. J.*, 2003, **35**, 93.

3. A. Comotti, S. Bracco, M. Beretta, J. Perego, M. Gemmi and P. Sozzani, *Chem. - Eur. J.*, 2015, **21**, 18209-18217.
4. O. M. Yaghi, M. O'Keeffe, N. W. Ockwig, H. K. Chae, M. Eddaoudi and J. Kim, *Nature*, 2003, **423**, 705.
5. S. Kitagawa, R. Kitaura and S.-i. Noro, *Angew. Chem. Int. Ed.*, 2004, **43**, 2334-2375.
6. G. Férey and C. Serre, *Chem. Soc. Rev.*, 2009, **38**, 1380-1399.
7. K. Sumida, D. L. Rogow, J. A. Mason, T. M. McDonald, E. D. Bloch, Z. R. Herm, T.-H. Bae and J. R. Long, *Chem. Rev.*, 2012, **112**, 724-781.
8. L. E. Kreno, K. Leong, O. K. Farha, M. Allendorf, R. P. Van Duyne and J. T. Hupp, *Chem. Rev.*, 2012, **112**, 1105-1125.
9. J.-R. Li, R. J. Kuppler and H.-C. Zhou, *Chem. Soc. Rev.*, 2009, **38**, 1477-1504.
10. P. Horcajada, R. Gref, T. Baati, P. K. Allan, G. Maurin, P. Couvreur, G. Férey, R. E. Morris and C. Serre, *Chem. Rev.*, 2012, **112**, 1232-1268.
11. T. Uemura, K. Kitagawa, S. Horike, T. Kawamura, S. Kitagawa, M. Mizuno and K. Endo, *Chem. Commun.*, 2005, 5968-5970.
12. T. S. Koblenz, J. Wassenaar and J. N. H. Reek, *Chem. Soc. Rev.*, 2008, **37**, 247-262.
13. S. Mochizuki, N. Ogiwara, M. Takayanagi, M. Nagaoka, S. Kitagawa and T. Uemura, *Nat. Commun.*, 2018, **9**, 329.
14. J. Lee, O. K. Farha, J. Roberts, K. A. Scheidt and S. T. Nguyen, *Chem. Soc. Rev.*, 2009, **38**, 1450-1459.
15. J. Liu, L. Chen, H. Cui, J. Zhang and L. Zhang, *Chem. Soc. Rev.*, 2014, **43**, 6011-6061.
16. M. Yoon, R. Srirambalaji and K. Kim, *Chem. Rev.*, 2012, **112**, 1196-1231.
17. N. Yanai, T. Uemura, M. Ohba, Y. Kadowaki, M. Maesato, M. Takenaka, S. Nishitsuji, H. Hasegawa and S. Kitagawa, *Angew. Chem. Int. Ed.*, 2008, **47**, 9883-9886.
18. T. Uemura, Y. Kadowaki, N. Yanai and S. Kitagawa, *Chem. Mater.*, 2009, **21**, 4096-4098.
19. C. J. Chuck, M. G. Davidson, M. D. Jones, G. Kociok-Köhn, M. D. Lunn and S. Wu, *Inorg. Chem.*, 2006, **45**, 6595-6597.
20. H. L. Nguyen, F. Gándara, H. Furukawa, T. L. H. Doan, K. E. Cordova and O. M. Yaghi, *J. Am. Chem. Soc.*, 2016, **138**, 4330-4333.
21. H. L. Nguyen, T. T. Vu, D. Le, T. L. H. Doan, V. Q. Nguyen and N. T. S. Phan, *ACS Catal.*, 2017, **7**, 338-342.
22. H.-C. Lee, M. Antonietti and B. V. K. J. Schmidt, *Polym. Chem.*, 2016, **7**, 7199-7203.
23. B. Liu, S. Jie, Z. Bu and B.-G. Li, *J. Mol. Catal. A: Chem.*, 2014, **387**, 63-68.
24. M. J. Vitorino, T. Devic, M. Tromp, G. Férey and M. Visseaux, *Macromol. Chem. Phys.*, 2009, **210**, 1923-1932.
25. R. C. Klet, S. Tussupbayev, J. Borycz, J. R. Gallagher, M. M. Stalzer, J. T. Miller, L. Gagliardi, J. T. Hupp, T. J. Marks, C. J. Cramer, M. Delferro and O. K. Farha, *J. Am. Chem. Soc.*, 2015, **137**, 15680-15683.
26. P. Ji, J. B. Solomon, Z. Lin, A. Johnson, R. F. Jordan and W. Lin, *J. Am. Chem. Soc.*, 2017, **139**, 11325-11328.
27. H. Li, B. Xu, J. He, X. Liu, W. Gao and Y. Mu, *Chem. Commun.*, 2015, **51**, 16703-16706.
28. R. J. Comito, K. J. Fritzsching, B. J. Sundell, K. Schmidt-Rohr and M. Dincă, *J. Am. Chem. Soc.*, 2016, **138**, 10232-10237.
29. R. J. C. Dubey, R. J. Comito, Z. Wu, G. Zhang, A. J. Rieth, C. H. Hendon, J. T. Miller and M. Dincă, *J. Am. Chem. Soc.*, 2017, **139**, 12664-12669.
30. J. Zhang, F. Dumur, P. Horcajada, C. Livage, P. Xiao, J. P. Fouassier, D. Gigmes and J. Lalevée, *Macromol. Chem. Phys.*, 2016, **217**, 2534-2540.
31. R. J. Comito, Z. Wu, G. Zhang, J. A. Lawrence, M. D. Korzyński, J. A. Kehl, J. T. Miller and M. Dincă, *Angew. Chem. Int. Ed.*, 2018, **57**, 8135-8139.
32. H.-C. Lee, M. Fantin, M. Antonietti, K. Matyjaszewski and B. V. K. J. Schmidt, *Chem. Mater.*, 2017, **29**, 9445-9455.
33. T. Uemura, R. Kitaura, Y. Ohta, M. Nagaoka and S. Kitagawa, *Angew. Chem. Int. Ed.*, 2006, **45**, 4112-4116.
34. H. Xing, D. Chen, X. Li, Y. Liu, C. Wang and Z. Su, *RSC Adv.*, 2016, **6**, 66444-66450.
35. X. Li, D. Chen, Y. Liu, Z. Yu, Q. Xia, H. Xing and W. Sun, *CrystEngComm*, 2016, **18**, 3696-3702.
36. Y. Liu, D. Chen, X. Li, Z. Yu, Q. Xia, D. Liang and H. Xing, *Green Chem.*, 2016, **18**, 1475-1481.
37. T. Ishiwata, Y. Furukawa, K. Sugikawa, K. Kokado and K. Sada, *J. Am. Chem. Soc.*, 2013, **135**, 5427-5432.
38. T. Ishiwata, K. Kokado and K. Sada, *Angew. Chem. Int. Ed.*, 2017, **56**, 2608-2612.
39. T. Uemura, Y. Ono, K. Kitagawa and S. Kitagawa, *Macromolecules*, 2008, **41**, 87-94.
40. J. Hwang, H.-C. Lee, M. Antonietti and B. V. K. J. Schmidt, *Polym. Chem.*, 2017, **8**, 6204-6208.
41. G. Moad, E. Rizzardo and S. H. Thang, *Aust. J. Chem.*, 2005, **58**, 379-410.
42. G. Moad, E. Rizzardo and S. H. Thang, *Aust. J. Chem.*, 2009, **62**, 1402-1472.
43. M. Kamigaito, T. Ando and M. Sawamoto, *Chem. Rev.*, 2001, **101**, 3689-3746.
44. V. Coessens, T. Pintauer and K. Matyjaszewski, *Prog. Polym. Sci.*, 2001, **26**, 337-377.
45. K. Matyjaszewski, *Macromolecules*, 2012, **45**, 4015-4039.
46. W. Jiang, X. Wang, J. Chen, Y. Liu, H. Han, Y. Ding, Q. Li and J. Tang, *ACS Appl. Mater. Interfaces*, 2017, **9**, 26948-26957.
47. Q. Fu, H. Ranji-Burachaloo, M. Liu, T. G. McKenzie, S. Tan, A. Reyhani, M. D. Nothling, D. E. Dunstan and G. G. Qiao, *Polym. Chem.*, 2018, **9**, 4448-4454.
48. M. Minagawa, T. Taira, Y. Yabuta, K. Nozaki and F. Yoshii, *Macromolecules*, 2001, **34**, 3679-3683.
49. F. E. Karasz and W. J. MacKnight, *Macromolecules*, 1968, **1**, 537-540.
50. C. De Rosa, F. Auriemma, A. Di Capua, L. Resconi, S. Guidotti, I. Camurati, I. E. Nifant'ev and I. P. Laishevtsev, *J. Am. Chem. Soc.*, 2004, **126**, 17040-17049.
51. Y. Isobe, D. Fujioka, S. Habaue and Y. Okamoto, *J. Am. Chem. Soc.*, 2001, **123**, 7180-7181.
52. K. Yamada, T. Nakano and Y. Okamoto, *Macromolecules*, 1998, **31**, 7598-7605.
53. J.-F. Lutz, W. Jakubowski and K. Matyjaszewski, *Macromol. Rapid Commun.*, 2004, **25**, 486-492.
54. T. Nakano, M. Mori and Y. Okamoto, *Macromolecules*, 1993, **26**, 867-868.
55. N. A. Porter, T. R. Allen and R. A. Breyer, *J. Am. Chem. Soc.*, 1992, **114**, 7676-7683.
56. T. Fujita and S. Yamago, *Chem. - Eur. J.*, 2015, **21**, 18547-18550.
57. H.-C. Lee, J. Hwang, U. Schilde, M. Antonietti, K. Matyjaszewski and B. V. K. J. Schmidt, *Chem. Mater.*, 2018, **30**, 2983-2994.

58. T. Uemura, Y. Ono, Y. Hijikata and S. Kitagawa, *J. Am. Chem. Soc.*, 2010, **132**, 4917-4924.
59. T. Uemura, N. Uchida, M. Higuchi and S. Kitagawa, *Macromolecules*, 2011, **44**, 2693-2697.
60. K. Osakada and D. Takeuchi, in *Polymer Synthesis*, Springer Berlin Heidelberg, Berlin, Heidelberg, 2004, pp. 137-194.
61. G. Ricci and G. Leone, *Polyolefins J.*, 1999, **1**, 43-60.
62. M. Kamachi and A. Kajiwara, *Macromolecules*, 1996, **29**, 2378-2382.
63. T. Uemura, R. Nakanishi, S. Mochizuki, Y. Murata and S. Kitagawa, *Chem. Commun.*, 2015, **51**, 9892-9895.
64. Y. Kobayashi, K. Honjo, S. Kitagawa, J. Gwyther, I. Manners and T. Uemura, *Chem. Commun.*, 2017, **53**, 6945-6948.
65. A. Matsumoto and T. Odani, *Macromol. Rapid Commun.*, 2001, **22**, 1195-1215.
66. K. Biradha and R. Santra, *Chem. Soc. Rev.*, 2013, **42**, 950-967.
67. J. W. Colson and W. R. Dichtel, *Nat. Chem.*, 2013, **5**, 453.
68. J. W. Lauher, F. W. Fowler and N. S. Goroff, *Acc. Chem. Res.*, 2008, **41**, 1215-1229.
69. I. H. Park, A. Chanthapally, Z. Zhang, S. S. Lee, M. J. Zaworotko and J. J. Vittal, *Angew. Chem. Int. Ed.*, 2014, **53**, 414-419.
70. I.-H. Park, A. Chanthapally, H.-H. Lee, H. S. Quah, S. S. Lee and J. J. Vittal, *Chem. Commun.*, 2014, **50**, 3665-3667.
71. I. H. Park, R. Medishetty, H. H. Lee, C. E. Mulijanto, H. S. Quah, S. S. Lee and J. J. Vittal, *Angew. Chem. Int. Ed.*, 2015, **54**, 7313-7317.
72. G. M. J. Schmidt, *Pure Appl. Chem.*, 1971, **27**, 647.
73. S.-Y. Yang, X.-L. Deng, R.-F. Jin, P. Naumov, M. K. Panda, R.-B. Huang, L.-S. Zheng and B. K. Teo, *J. Am. Chem. Soc.*, 2014, **136**, 558-561.
74. H. J. Harwood, *Makromol. Chem., Macromol. Symp.*, 1987, **10-11**, 331-354.
75. H. Hirai, *J. Polym. Sci. Macromol. Rev.*, 1976, **11**, 47-91.
76. Y. Hibi, S. Tokuoka, T. Terashima, M. Ouchi and M. Sawamoto, *Polym. Chem.*, 2011, **2**, 341-347.
77. Y. Hibi, M. Ouchi and M. Sawamoto, *Angew. Chem. Int. Ed.*, 2011, **50**, 7434-7437.
78. M. Ouchi, M. Nakano, T. Nakanishi and M. Sawamoto, *Angew. Chem. Int. Ed.*, 2016, **55**, 14584-14589.
79. T. Uemura, Y. Ono and S. Kitagawa, *Chem. Lett.*, 2008, **37**, 616-617.
80. T. Uemura, S. Mochizuki and S. Kitagawa, *ACS Macro Lett.*, 2015, **4**, 788-791.
81. T. Uemura, D. Hiramatsu, Y. Kubota, M. Takata and S. Kitagawa, *Angew. Chem. Int. Ed.*, 2007, **46**, 4987-4990.
82. T. Uemura, R. Nakanishi, T. Kaseda, N. Uchida and S. Kitagawa, *Macromolecules*, 2014, **47**, 7321-7326.
83. Y. Kobayashi, Y. Horie, K. Honjo, T. Uemura and S. Kitagawa, *Chem. Commun.*, 2016, **52**, 5156-5159.
84. F. S. Bates and G. H. Fredrickson, *Phys. Today*, 1999, **52**, 32-38.
85. H. Nishida and Y. Tokiwa, *J. Appl. Polym. Sci.*, 1992, **46**, 1467-1476.
86. H. G. Börner, *Prog. Polym. Sci.*, 2009, **34**, 811-851.
87. R. Arshady, *Colloid. Polym. Sci.*, 1992, **270**, 717-732.
88. J. P. Rao and K. E. Geckeler, *Prog. Polym. Sci.*, 2011, **36**, 887-913.
89. L. Katharina, *Angew. Chem. Int. Ed.*, 2009, **48**, 4488-4507.
90. R. Arshady and M. H. George, *Polym. Eng. Sci.*, 1993, **33**, 865-876.
91. P. Yang, T. Deng, D. Zhao, P. Feng, D. Pine, B. F. Chmelka, G. M. Whitesides and G. D. Stucky, *Science*, 1998, **282**, 2244-2246.
92. P. Jiang, J. F. Bertone and V. L. Colvin, *Science*, 2001, **291**, 453-457.
93. P. Sozzani, S. Bracco, A. Comotti, R. Simonutti, P. Valsesia, Y. Sakamoto and O. Terasaki, *Nat. Mater.*, 2006, **5**, 545.
94. N. Stock and S. Biswas, *Chem. Rev.*, 2012, **112**, 933-969.
95. A. Umemura, S. Diring, S. Furukawa, H. Uehara, T. Tsuruoka and S. Kitagawa, *J. Am. Chem. Soc.*, 2011, **133**, 15506-15513.
96. V. Safarifard and A. Morsali, *Coord. Chem. Rev.*, 2015, **292**, 1-14.
97. J. Hwang, T. Heil, M. Antonietti and B. V. K. J. Schmidt, *J. Am. Chem. Soc.*, 2018, **140**, 2947-2956.
98. Y. Lu, Y. Yin and Y. Xia, *Adv. Mater.*, 2001, **13**, 415-420.
99. Y. Lu, Y. Yin, Z.-Y. Li and Y. Xia, *Langmuir*, 2002, **18**, 7722-7727.
100. J. A. Champion, Y. K. Katare and S. Mitragotri, *J. Controlled Release*, 2007, **121**, 3-9.
101. R. Arshady, *Polym. Eng. Sci.*, 1989, **29**, 1746-1758.
102. T. Uemura, T. Kaseda and S. Kitagawa, *Chem. Mater.*, 2013, **25**, 3772-3776.
103. T. Uemura, N. Uchida, A. Asano, A. Saeki, S. Seki, M. Tsujimoto, S. Isoda and S. Kitagawa, *J. Am. Chem. Soc.*, 2012, **134**, 8360-8363.
104. T. Kitao, M. W. A. MacLean, B. Le Ouay, Y. Sasaki, M. Tsujimoto, S. Kitagawa and T. Uemura, *Polym. Chem.*, 2017, **8**, 5077-5081.
105. T. Wang, M. Farajollahi, S. Henke, T. Zhu, S. R. Bajpe, S. Sun, J. S. Barnard, J. S. Lee, J. D. W. Madden, A. K. Cheetham and S. K. Smoukov, *Mater. Horiz.*, 2017, **4**, 64-71.
106. C. Lu, T. Ben, S. Xu and S. Qiu, *Angew. Chem. Int. Ed.*, 2014, **53**, 6454-6458.
107. Q. X. Wang and C. Y. Zhang, *Macromol. Rapid Commun.*, 2011, **32**, 1610-1614.
108. Z.-G. Gu, W.-Q. Fu, M. Liu and J. Zhang, *Chem. Commun.*, 2017, **53**, 1470-1473.
109. M. F. Toney, T. P. Russell, J. A. Logan, H. Kikuchi and J. M. Sands, *Nature*, 1995, **374**, 709-711.
110. N. Naga, Y. Saito, K. Noguchi, K. Takahashi, K. Watanabe and M. Yamato, *Polym. J.*, 2016, **48**, 709.
111. M. Richard-Lacroix and C. Pellerin, *Macromolecules*, 2013, **46**, 9473-9493.
112. T. Uemura, S. Horike, K. Kitagawa, M. Mizuno, K. Endo, S. Bracco, A. Comotti, P. Sozzani, M. Nagaoka and S. Kitagawa, *J. Am. Chem. Soc.*, 2008, **130**, 6781-6788.
113. T. Uemura, N. Yanai, S. Watanabe, H. Tanaka, R. Numaguchi, M. T. Miyahara, Y. Ohta, M. Nagaoka and S. Kitagawa, *Nat. Commun.*, 2010, **1**, 83.
114. T. Kitao, S. Bracco, A. Comotti, P. Sozzani, M. Naito, S. Seki, T. Uemura and S. Kitagawa, *J. Am. Chem. Soc.*, 2015, **137**, 5231-5238.
115. G. Distefano, H. Suzuki, M. Tsujimoto, S. Isoda, S. Bracco, A. Comotti, P. Sozzani, T. Uemura and S. Kitagawa, *Nat. Chem.*, 2013, **5**, 335-341.
116. M. Li, C. Ma, X. Liu, J. Su, X. Cui and Y. He, *Chem. Sci.*, 2018, **9**, 5912-5918.

117. L. Xia, Z. Wei and M. Wan, *J. Colloid Interface Sci.*, 2010, **341**, 1-11.
118. G. Cheng, C. Youchun, Z. Zhongbo, X. Shanfeng, S. Shuheng, Z. Chengmei, Z. Huanhuan, L. Ying, L. Fenghong, H. Fei and M. Yuguang, *Adv. Energy Mater.*, 2014, **4**, 1301771.
119. K. Yan, X. Yanhong, G. Zhaoqi and J. Donglin, *Angew. Chem. Int. Ed.*, 2011, **50**, 8753-8757.
120. T. Mehling, I. Smirnova, U. Guenther and R. H. H. Neubert, *J. Non-Cryst. Solids*, 2009, **355**, 2472-2479.
121. T. A. Debele, S. L. Mekuria and H.-C. Tsai, *Mater. Sci. Eng., C*, 2016, **68**, 964-981.
122. Y. Kobayashi, K. Honjo, S. Kitagawa and T. Uemura, *ACS Appl. Mater. Interfaces*, 2017, **9**, 11373-11379.
123. K. Jindřich and Y. Jiyuan, *Polym. Int.*, 2007, **56**, 1078-1098.
124. L. L. Hench and I. Thompson, *J. R. Soc. Interface*, 2010, **7**, S379-S391.
125. M. Shibayama, S.-i. Takata and T. Norisuye, *Physica A*, 1998, **249**, 245-252.
126. Y. Furukawa, T. Ishiwata, K. Sugikawa, K. Kokado and K. Sada, *Angew. Chem. Int. Ed.*, 2012, **51**, 10566-10569.
127. K. Kokado, T. Ishiwata, S. Anan and K. Sada, *Polym. J.*, 2017, **49**, 685-689.
128. M. Tsotsalas, J. Liu, B. Tettmann, S. Grosjean, A. Shahnas, Z. Wang, C. Azucena, M. Addicoat, T. Heine, J. Lahann, J. Overhage, S. Bräse, H. Gliemann and C. Wöll, *J. Am. Chem. Soc.*, 2014, **136**, 8-11.
129. S. Schmitt, M. Silvestre, M. Tsotsalas, A.-L. Winkler, A. Shahnas, S. Grosjean, F. Laye, H. Gliemann, J. Lahann, S. Bräse, M. Franzreb and C. Wöll, *ACS Nano*, 2015, **9**, 4219-4226.
130. S. Schmitt, J. Hümmer, S. Kraus, A. Welle, S. Grosjean, M. Hanke-Roos, A. Rosenhahn, S. Bräse, C. Wöll, C. Lee-Thedieck and M. Tsotsalas, *Adv. Funct. Mater.*, 2016, **26**, 8455-8462.
131. Z. Wang, A. Błaszczyk, O. Fuhr, S. Heissler, C. Wöll and M. Mayor, *Nat. Commun.*, 2017, **8**.
132. D. R. Paul and C. B. Bucknall, *Polymer blends*, 1999.
133. K. F. Freed and J. Dudowicz, in *Phase Behaviour of Polymer Blends*, ed. K. F. Freed, Springer Berlin Heidelberg, Berlin, Heidelberg, 2005, pp. 63-126.
134. T. Uemura, T. Kaseda, Y. Sasaki, M. Inukai, T. Toriyama, A. Takahara, H. Jinnai and S. Kitagawa, *Nat. Commun.*, 2015, **6**.